Signatures of lateral coupling of double quantum dots in the exciton photoluminescence spectrum

B. Szafran[1,2] and F. M. Peeters[2]
[1]*Faculty of Physics and Applied Computer Science, AGH University of Science and Technology, Aleja Mickiewicza 30, 30-059 Kraków, Poland*
[2]*Departement Fysica, Universiteit Antwerpen, Groenenborgerlaan 171, B-2020 Antwerpen, Belgium*
(Received 16 July 2007; published 28 November 2007)

We study an electron-hole pair in laterally coupled self-assembled quantum dots with an electric field applied in the plane of confinement. The interparticle correlations and the carrier distribution are calculated using a configuration interaction approach for dots with circular and square symmetry. We extract universal features of the photoluminescence spectra specific to the lateral coupling configuration and point out the differences with vertically coupled dots. These specific features include additional avoided crossings of the lowest bright exciton level as function of the external field. In the case of strong coupling, the avoided crossing related to exciton dissociation is anomalous and involves an interaction of three or four energy levels. The latter is a consequence of the hole state mixing appearing at the electron transfer between the dots.

DOI: 10.1103/PhysRevB.76.195442 PACS number(s): 73.21.La, 73.43.−f, 71.10.Pm

I. INTRODUCTION

In vertically stacked quantum dots the carriers form artificial molecular orbitals that can be intentionally tuned by an external electric field. Field-induced exciton dissociation was observed in photoluminescence experiments.[1–4] The dissociation by the removal of the electron from the dot occupied by the hole results in an avoided crossing of a bright and a dark energy level, which is a signature of the interdot electron tunnel coupling.[1–11]

Recently, fabrication of planar structures containing two[12] or more[13–15] laterally coupled dots was reported.[16] The electron coupling in planar double-dot structures was observed in the photoluminescence spectrum.[12] The purpose of the present paper is to investigate the exciton coupling in laterally coupled dots when the electric field is applied within the plane of confinement. We determine features in the photoluminescence spectrum which are characteristic for lateral coupling.

For vertically stacked structures, the spectral effects related to the interdot carrier transfer turn out to be essentially independent of the details of the confinement in the separate dots.[10] The interdot electron transfer is induced by a vertical electric field varying by about 10 kV/cm.[10] In such a field range, the wave functions of the separate dots are not significantly perturbed due to the strong vertical confinement in the dots. We show below that for lateral coupling, the electric field needed to transfer the carriers between the dots will visibly deform the wave functions within each of the dots and mix the single-dot energy levels. The details of the in-plane confinement are therefore likely to influence the spectra in a more pronounced manner. To extract universal features for the lateral coupling, we consider dots both of circular and square symmetries.

In the present paper, we employ the approach previously developed to describe electron and hole localization in vertically stacked dots.[7,10] This approach incorporates the electron-hole correlations that are tuned by the external field. Such an approach turned out to be successful in predicting the dissociation mechanisms of both the exciton[1–3] and negative trion[4] in asymmetric double dots (see also Sec. I of Ref. 10). We note that a configuration interaction approach was recently applied[17] to describe the exciton states in laterally coupled dots but in the absence of an electric field.

The paper is organized as follows. In Sec. II, the model is briefly described, and the results are given in Sec. III and discussed in Sec. IV. Section V contains the summary and our conclusions.

II. MODEL

We adapt the model and computational approach of our previous paper[10] originally applied to InGaAs vertically stacked dots. The model applies the single band approximation for the hole, which is justified by the flat geometry of the self-assembled quantum dots reducing the light hole contribution to the lowest energy states. We neglect spin effects (electron-hole exchange and fine structure splitting) which are crucial for the photon polarization but small in the energy scale of the effects that arise due to the interdot carrier transfer.

The exciton Hamiltonian is diagonalized within the configuration interaction approach with the single carrier functions obtained in a multicenter Gaussian basis,[10] which allows for an exact treatment of the electron-hole correlations in arbitrarily complex structures without any assumptions on the potential symmetry or electric-field direction.

We use the material parameters of Ref. 10 and apply similar confinement models for the three-dimensional quantum wells with smooth walls. The confinement potential in our coupled quantum dots is modeled by (see Fig. 1)

$$V(x,y,z) = -\left[\frac{V^l}{1+\left(\frac{(x-d/2)^2+y^2}{R^2}\right)^{40}} + \frac{V^r}{1+\left(\frac{(x+d/2)^2+y^2}{R^2}\right)^{40}}\right]\frac{1}{\left(1+\left(\frac{z}{Z}\right)^{20}\right)}, \quad (1)$$

for the circular dots, and

$$V(x,y,z) = -\left[\frac{V^l}{1+\left(\frac{(x-d/2)^2}{a^2}\right)^{40}+\left(\frac{y^2}{a^2}\right)^{40}} + \frac{V^r}{1+\left(\frac{(x+d/2)^2}{a^2}\right)^{40}+\left(\frac{y^2}{a^2}\right)^{40}}\right]\frac{1}{\left(1+\left(\frac{z}{Z}\right)^{20}\right)}, \quad (2)$$

for the square dots. $2Z=4$ nm is the height of the dot, and the disk diameter ($2R$) and the side length of the square dot ($2a$) are taken equal to 20 nm. In formulas (1) and (2), d is the distance between the dot centers (see Fig. 1), and V^l and V^r are the depths of the potential well in the left and right dots, respectively. To account for the inevitable asymmetry, in our approach[10] the left dot is assumed deeper by 10 meV for both the electron and the hole (for the discussion of the two separate cases, which turn out to be equivalent due to the interaction, see Ref. 7).

For completeness, at the end of Sec. III, we consider a system of square dots without a common symmetry axis, i.e., dots that are displaced with respect to each other in the y direction.

III. RESULTS

A. Single square quantum dot

For our discussion of coupled square dots, it is useful to begin by evaluation of effects originating from a single dot.

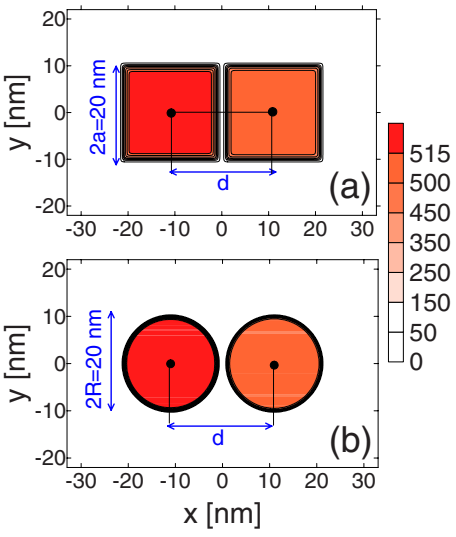

FIG. 1. (Color online) Top view [cross section ($z=0$)] of the electron confinement potential [Eqs. (1) and (2)] for the laterally coupled dots with (a) square or (b) circular disk shape. Colors stand for the depth of the electron confinement (scale given at the right of the figure in meV). The left dot is deeper by 10 meV.

Figure 2 shows the variation of the ground-state energy when the electric field $F=20$ kV/cm is rotated from the x to the y direction [$\mathbf{F}=(F\cos\phi, F\sin\phi)$], from $\phi=0$ to $\phi=\pi/2$. This field is strong enough to visibly deform the hole charge density (see the insets), and the electron is only slightly affected. The ground-state energy is lowered by the field when it separates the carriers. Therefore, it is minimal when the field is oriented along the diagonal of the square. The uppermost inset corresponds to $\phi=0$, the middle one to $\phi=\pi/4$, and the lowest to $\phi=\pi/8$. Recombination probability[10] falls by about 4% when the field is switched from the $x=0$ to the $y=x$ (diagonal) direction. At $F=20$ kV/cm, the ground-state energy changes by only 0.3 meV when the field vector is rotated within the plane of confinement.

B. Laterally coupled square quantum dots

For the laterally coupled double dot, we first consider the electric field oriented parallel to the x axis, $\mathbf{F}=(F_x,0)$. The F_x dependence of the energy spectrum is presented in Fig. 3(a) for $d=21$ nm and in Fig. 3(b) for $d=20$ nm. In Fig. 3, the width of the curves is set proportional to the recombination probability calculated for the exciton state with wave function ϕ as

$$p = \left|\int d^6\mathbf{r}\,\phi(\mathbf{r}_e,\mathbf{r}_h)\,\delta^3(\mathbf{r}_e-\mathbf{r}_h)\right|^2. \quad (3)$$

In the plots, we observe two bright[18] energy levels (the thick curves) that depend on the field in a parabolic fashion. The two bright levels are crossed or avoided crossed by dark energy levels with spatially separated electron and hole. Dependence of these levels on the field is much stronger and nearly linear.

The electron and hole densities corresponding to the energy levels in Fig. 3(a) are plotted in Fig. 4. At $F=0$, the ground state (α) is completely localized in the left (deeper) dot [see Fig. 4(a)], while in the excited state (β), the carriers are localized in the right (shallower) dot. For the β state, we spot a trace of electron tunneling to the left dot (higher energy corresponds to stronger tunneling).

In the lower bright energy level, two avoided crossings are observed at $F_x>0$. A similar pattern (nearly a mirror reflection) of avoided crossings is observed in the upper bright state at $F_x<0$. In the lower bright state, $F_x>0$ tends to shift the electron from the left to the right dot, while in the

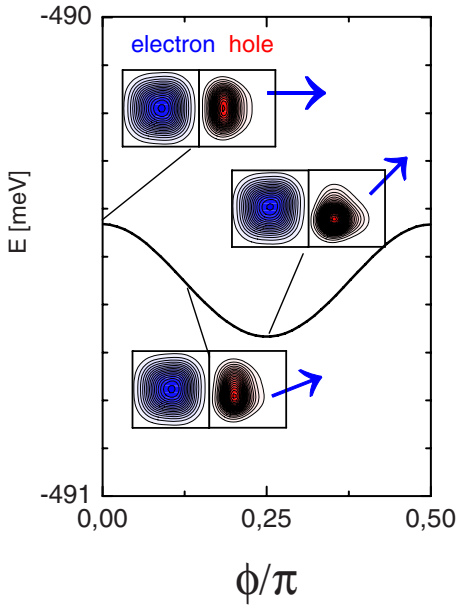

FIG. 2. (Color online) Ground-state exciton energy for a single square quantum dot (the left, deeper one of the model) as function of electric-field orientation for $F=20$ kV/cm. The plot contains three double insets. In each inset, left (right) panel shows the contour plot of the electron (hole) density cross section at $z=0$. The square frame shows the nominal dot dimensions of $2a=20$ nm. The arrows indicate the direction of the electric field acting on the electron.

higher bright state, negative F_x is needed to transfer the electron from the right to the left dot. In the following, we focus on the electron localization in the lowest bright energy level. At $F_x=13$ kV/cm, the first avoided crossings is obtained [see the points marked by γ and δ in Fig. 3(a) and the carrier densities presented in Fig. 4(b)]. In the γ-δ avoided crossing, the hole is pushed to the left side of the left dot but the electron in the ground-state is transferred from the left to the right dot. After the avoided crossing, the ground state corresponds to spatially separated carriers and becomes dark.

For *vertical* quantum dots, the lowest bright energy level undergoes only a *single* avoided crossing, which is related to the exciton ground-state dissociation. However, for laterally coupled dots, we observe another avoided crossing appearing at higher electric field near $F=47$ kV/cm (energy levels marked by ϵ and ζ in Fig. 3). Figure 4(c) shows that at this anticrossing, the electron is transferred from its lowest energy level associated with the left dot to an excited electron energy level associated with the right dot. Mixing of these two electron levels is observed as the avoided crossing. The carrier distribution after the avoided crossings—when the mixing is no longer present—is displayed in Fig. 4(d) for $F=60$ kV/cm.

The multitude of dark energy levels observed in Fig. 3 is mostly due to the hole excitations, and only a few states with electron excitations are present in the plot. Besides the state participating in the ϵ-ζ avoided crossing, in the low part of the spectrum, we have the energy level marked by π in Fig. 3(a). This energy level corresponds to an electron excitation with wave function which changes sign along the $x=0$ line.

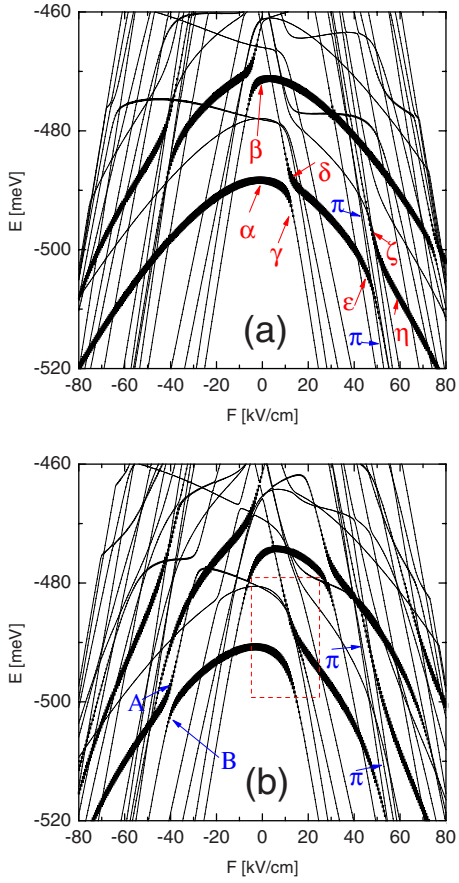

FIG. 3. (Color online) Exciton energy spectrum for two coupled square quantum dots. The square quantum dots are put side by side [centers are located at $(-d/2,0)$ and $(d/2,0)$] for (a) $d=21$ nm and (b) $d=20$ nm. Thickness of the lines is proportional to the recombination probability.

At $F=0$, the π energy level is degenerate with the one participating in the ϵ-ζ avoided crossing, which has a nodal surface perpendicular to the x axis.

The spectrum for stronger coupling with $d=20$ nm [see Fig. 3(b)] shows the appearance of additional characteristic features. $F_x<0$ stabilizes the electron in the left (deeper) dot but tends to remove the hole to the right one. Between 0 and −30 kV/cm, four energy levels cross or nearly cross the lowest bright energy level. Near $F_x=-40$ kV/cm, a much wider avoided crossing is obtained [see anticrossing energy levels marked by A and B in Fig. 3(b)]. This avoided crossing is associated with the mixing of the lowest hole energy level of the left dot with an excited one of the right dot—see Fig. 5.

At a closer inspection, one notices that the ground-state exciton dissociation at $F=+15$ kV/cm has an unusual character. The zoom of the rectangle of Fig. 3(b) is presented in Fig. 6 which shows that the dissociation at $d=20$ nm appears with a *third* state involved in the avoided crossing. In all the energy levels presented in Fig. 6, the hole remains in the deeper dot (see Fig. 7). Only the electron is transferred by the field. The first excited state near 15 kV/cm is dark and corresponds to the hole wave function in the deeper dot with a nodal surface parallel to the field. At $F_x=15$ kV/cm in both second and third energy levels, the hole wave function is a

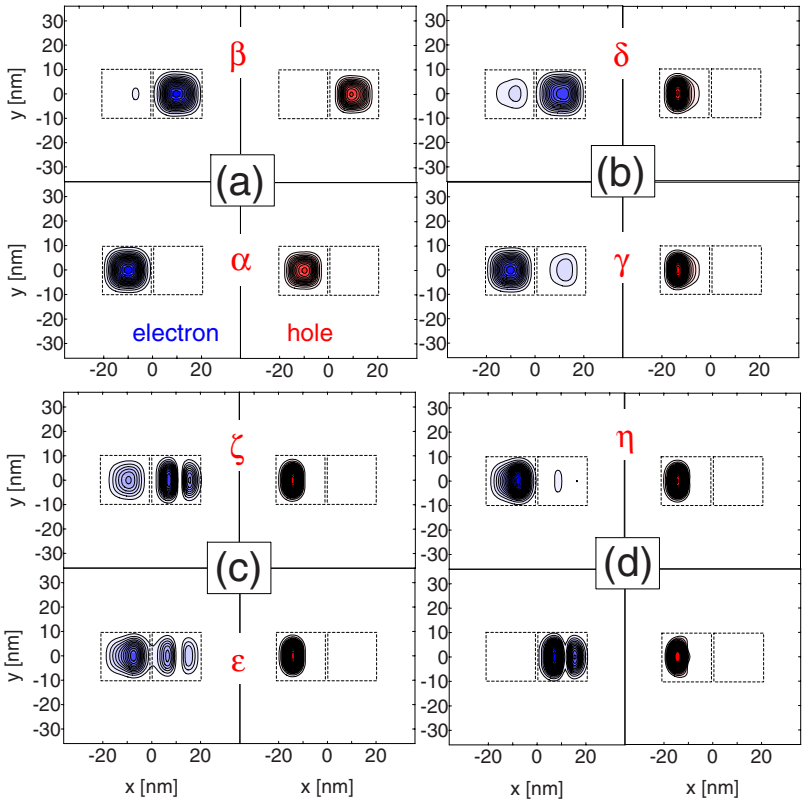

FIG. 4. (Color online) Electron (left panels, blue) and hole (right panels, red) charge densities for double square quantum dots with $d=21$ nm. Plots (a), (b), (c), and (d) correspond to $F=0,13,47,60$ kV/cm, respectively (positive electric field pushes the electron to the right and the hole to the left). The dotted lines show the nominal dot boundaries. The corresponding energy levels marked with the Greek letters are shown in Fig. 3(a).

superposition of the lowest-energy-level wave function with a wave function changing sign perpendicular to the field (see Fig. 7). As a result in both exciton states, the hole density has two maxima; the highest density is on the left dot where most of the electron charge is localized. The hole wave function mixing allows both these states to be bright at 15 kV/cm. Above 20 kV/cm when the electron is moved (see Fig. 7) to the shallower dot, the second excited state becomes dark due to the spatial carrier separation, and in the third excited state, admixture of the hole excitation disappears. The discussed anomaly of the complex avoided crossing is due to the hole energy level mixing induced by the interaction at the *electron transfer* between the dots.

C. Coupled circular dots

Figure 8 shows the electric-field dependence of the exciton energy spectrum for a double circular disk system with dot centers separated by 21 nm (a) and 20 nm (b) for the electric field vector oriented parallel to the x direction.[19] The effect of the dots shape on the spectra can be evaluated by comparing Fig. 8 to its counterpart for square dots presented in Fig. 3. For $d=21$ nm, a trace of the lateral coupling is visible in the energy level repulsion near the ground-state exciton dissociation at $F_x \simeq 12$ kV/cm. Similar narrow avoided crossing for the dissociation of the exciton localized in the shallower dot appears in the higher bright energy level near $F_x=-7$ kV/cm. More pronounced is the avoided crossing observed in the lower bright state near $F_x=70$ kV/cm [marked with a circle in Fig. 8(a)]. The corresponding electron densities for the energy levels participating in the avoided crossing are presented in Figs. 9(d) and 9(e). This avoided crossing is a counterpart of the ϵ-ζ anticrossing discussed above for the square dots.

Avoided crossings become wider at $d=20$ nm [see Fig. 8(b)] but remain much less pronounced than in the case of square dots [see Fig. 3(b)]. Note that a hole-tunneling-related avoided crossing is also visible near $F_x=-50$ kV/cm [marked with a circle in Fig. 8(b)] for the lower bright level and near $F_x=40$ kV/cm for the higher bright level. For the square quantum dots, the hole density at the avoided crossing

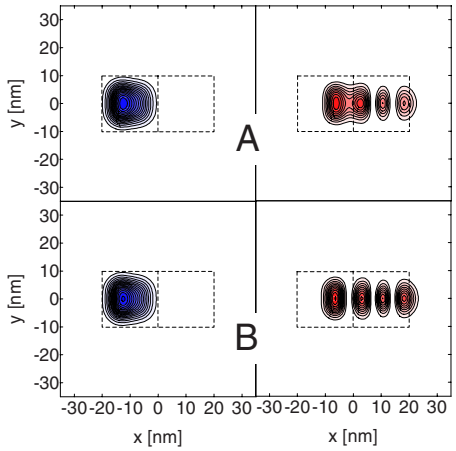

FIG. 5. (Color online) Electron (left panels) and hole (right panels) densities for square dots calculated at $F=-40$ kV/cm with a distance between the dot centers of 20 nm. The dotted lines show the nominal dot boundaries. Corresponding anticrossing energy levels marked by A and B are displayed in Fig. 3(b).

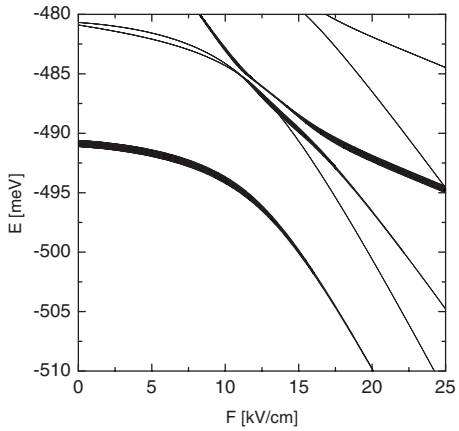

FIG. 6. Zoom of the rectangle of Fig. 3(b) for the anomalous ground-state exciton dissociation involving a third energy level in the avoided crossing.

had three extrema along the right dot axis [see Figs. 5(f) and 5(g)]. In the case of circular dots, the hole state which is responsible for the wide avoided crossing has multiple maxima at the edge of the right dot [see Fig. 9(b) and 9(c)] (it stems from a hole state of angular momentum $l=4\hbar$ in the absence of the field). The hole excitation which leads to stronger hole tunneling and, consequently, to a pronounced avoided crossing is therefore structure dependent.

D. Rotated electric field

Let us now discuss the effect of the rotation of the electric field on the spectra. Figure 10 corresponds to a field of $F=20$ kV/cm rotated within the x-y plane [$\mathbf{F}=(F\cos(\phi),F\sin(\phi))$], for circular disks [Fig. 10(a)] and square [Fig. 10(b)] dots.

In the ground state at $\phi=\pi/2$ (when the field is oriented perpendicular to the coupling direction), the electron and the hole occupy the deeper dot. For $\pi/2<\phi<3\pi/2$, the hole is pushed to the left (shallower dot). The ground state dissociation through an extremely narrow avoided crossing of energy levels (hole tunneling) is observed in both circular and square cases. For square dots, the width of the avoided crossing is of the order of 0.1 meV, and for circular dots, it is at most 10 μeV. For fixed distance between the dot centers, the width of the avoided crossings for circular dots is typically much smaller than for square dots, which is due to smaller contact area between the circular dots. For square dots, the interdot barrier thickness takes its minimal value on the entire side length of a square (see Fig. 1), while for circular dots, the thickness is minimal only at the line joining the dot centers.

On the other hand, at $-\pi/2<\phi<\pi/2$, the electric field tends to transfer the electron to the right dot. The transfer goes through a wide avoided crossing. Note that in Fig. 10(b), one observes an anomalous avoided crossing with an

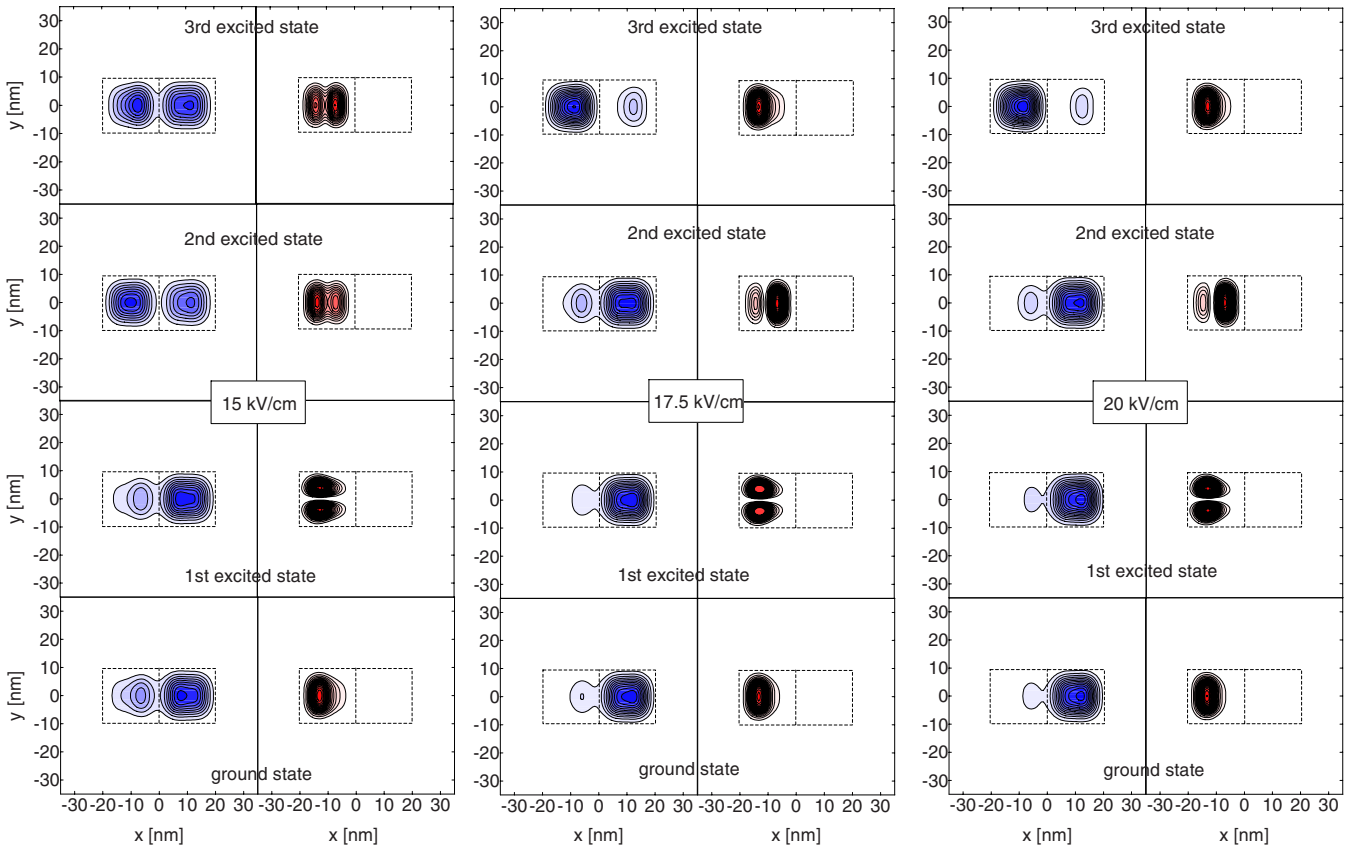

FIG. 7. (Color online) Electron (left of each pair of plots) and hole (the right one) densities in four lowest-energy states whose levels were presented in Fig. 6 at 15 kV/cm (left panel), 17.5 kV/cm (middle panel), and 20 kV/cm (right panel). The lower plots correspond to lower energies.

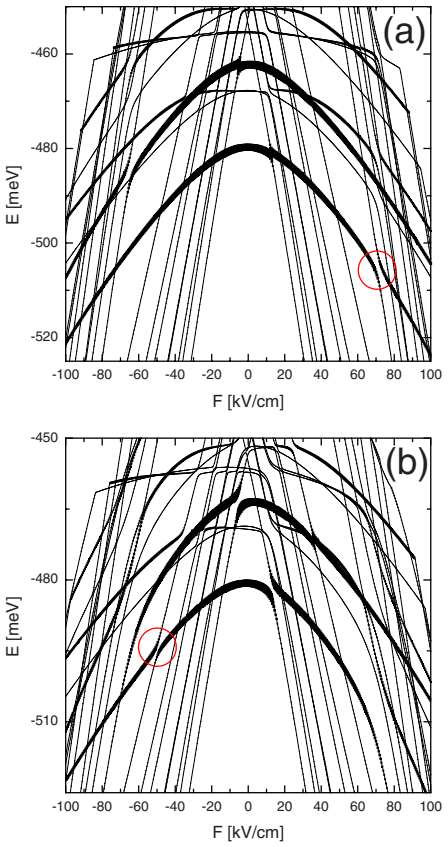

FIG. 8. (Color online) Same as Fig. 3 but for circular dots with the dot centers of (a) $d=21$ nm and (b) $d=20$ nm. The circles mark the avoided crossing discussed in the text.

extra third and fourth energy level. For aligned dots and the electric field oriented along the x direction, the anomalous avoided crossings (see Figs. 6 and 7) involves only three energy levels. Carrier densities are presented in Fig. 11 for $\phi=\pi/4$. For the x-field direction, the first excited state was associated with an excited hole with a nodal surface on the potential symmetry axis (see Fig. 7). For the rotated field, this is no longer the case and the state participates in the avoided crossing.

Note that the lowest bright energy level outside the avoided crossing is a flatter function of ϕ for the circular dots than for the square dots. It is the single square dot asymmetry effect presented in Fig. 2 which leads to the variation of the lowest bright energy level outside the avoided crossing. The overall effect of the asymmetry is qualitatively negligible compared to the effects of the electron transfer between the dots.

E. Misaligned square dots

We considered a pair of square dots with displaced symmetry axes [see inset of Fig. 12(a)]. The spectrum for the x-oriented field is plotted in Fig. 12(a) for centers of the dots shifted by 20 nm in the x direction and by 10 nm in the y direction. The shift in the y direction basically reduces the interdot coupling, and the spectrum resembles more the $d=21$ nm aligned case of Fig. 3(a) than the $d=20$ nm spectrum of Fig. 3(b). The spectrum for rotated electric field ($F=20$ kV/cm) is displayed in Fig. 12(b). Compared to the perfectly aligned case of Fig. 10(b), besides narrower avoided crossings, one observes that the spectrum loses

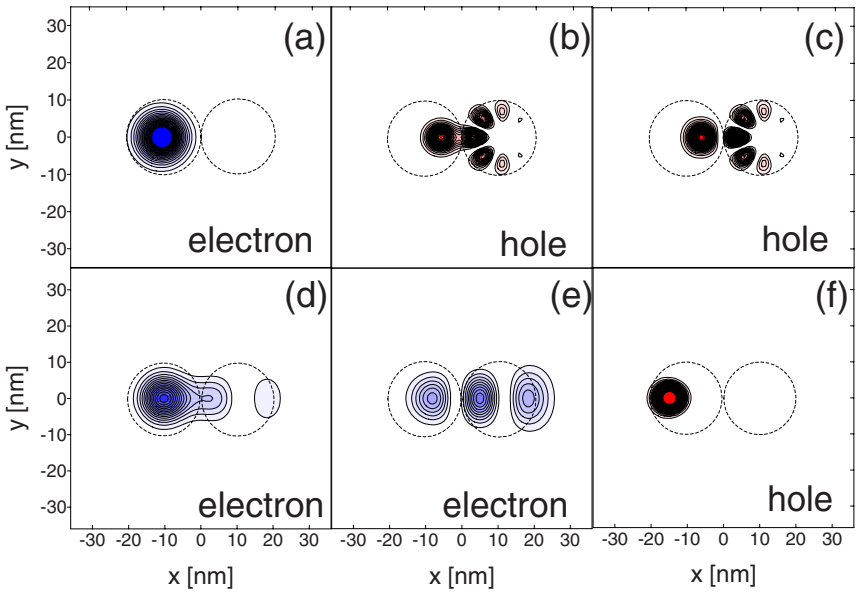

FIG. 9. (Color online) Electron and hole densities for circular dots with distances between the centers of $d=20$ nm [panels (a)–(c)] and $d=21$ nm [panel (d)–(f)]. Plots (a)–(c) were calculated at $F_x=-50$ kV/cm and correspond to the hole related avoided crossing marked by a circle in Fig. 8(b). Plots (d)–(f) were made for $F_x=70$ kV/cm and correspond to the electron avoided crossing marked by a circle in Fig. 8(a). For the hole avoided crossing, the electron density is nearly the same in both participating states (and vice versa). Plots (a), (b), (d), and (f) were made for the lower energy level of the anticrossing couples marked by circles in Fig. 8 and plots (c) and (e) for the higher energy level of each couple.

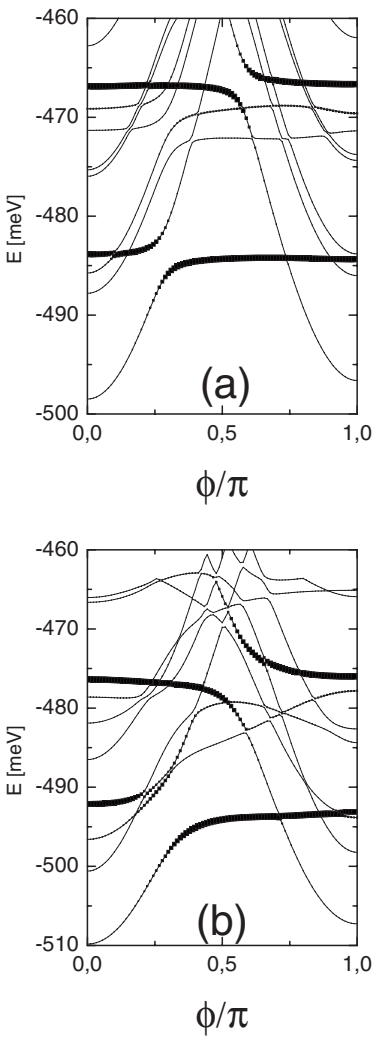

FIG. 10. Energy spectra for electric-field vector of length $F=20$ kV/cm rotated in the x-y plane $[F_x=F\cos(\phi), F_y=F\sin(\phi)]$ for (a) circular and (b) square dots with centers spaced by $d=20$ nm.

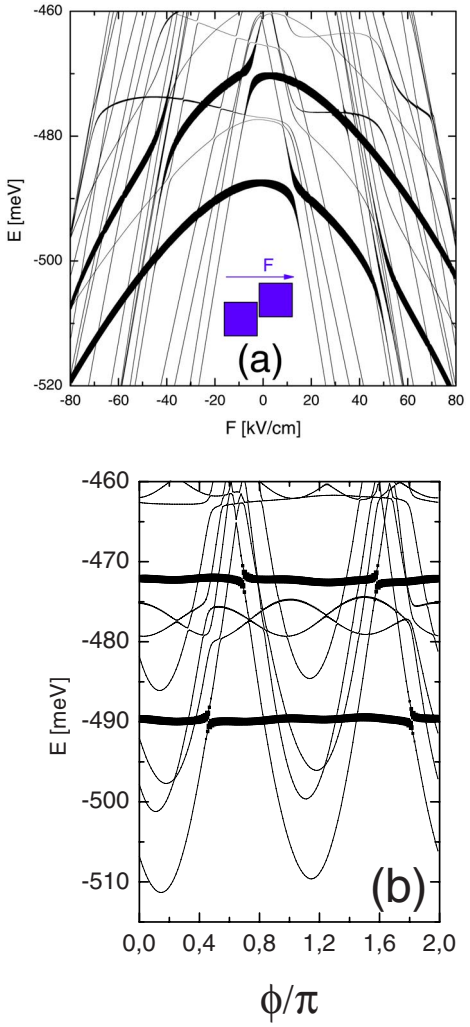

FIG. 12. (Color online) Spectrum for the square dots with centers separated by 20 nm in the x direction and by 10 nm in the y direction [see inset in (a)] as (a) function of the field oriented in the x direction and (b) for the field of $F=20$ kV/cm rotated within the plane of confinement.

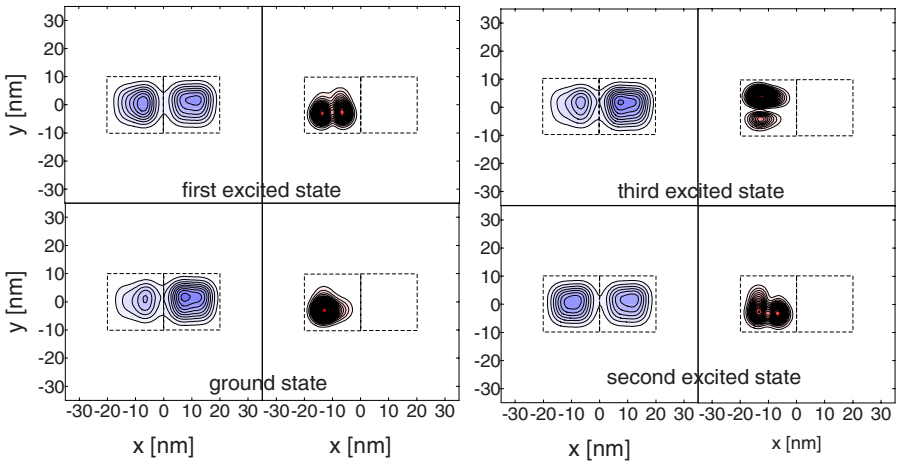

FIG. 11. (Color online) Contour plots of the electron (left panels) and hole (right panels) at $z=0$ plane for the square quantum dots at the electric field of 20 kV/cm oriented at $\phi=\pi/4$ angle. For $\phi=0$—see Fig. 7—the rightmost column of plots.

the local symmetry with respect to $\phi=0$ and $\phi=\pi$ field orientations.

IV. DISCUSSION

Let us discuss the presented results in the context of the thoroughly studied case of the exciton Stark effect in vertically coupled dots.[1–11]

For vertical dots, a distinct coupling is still observed at a barrier width of about 10 nm.[10] In the case of lateral coupling, the dots need nearly to touch each other in order to allow tunnel coupling. This is due to a smaller contact area of the laterally coupled potential cavities. For the same reason, the circular dots are much more difficult to couple laterally than the square dots.

The deformation of the wave functions by the in-plane electric field results in a single-dot polarizability[20] (defined as the second derivative of the energy level with respect to the field) being much stronger than for the vertical field orientation. To see this, compare the field dependence of the bright energy levels plotted in Figs. 3 and 8 with Fig. 2 of our previous paper[10] plotted in similar energy-field scales.

The features of the spectra specific to lateral coupling are the following: (1) In the vertically coupled dots, a single wide avoided crossing is observed for each of the two bright levels associated with both dots. On the other hand, in the case of lateral coupling for both circular and square dots, we demonstrated the appearance of an additional avoided crossings at higher electric fields which are related to the electron transfer to an excited energy level of the shallower dot (of approximate odd parity with respect to the dot center). The odd state of the shallower dot does not recombine with the hole localized in the deeper dot, but it interacts with the electron state of the deeper dot. For vertical quantum dots, an additional avoided crossing is excluded unless an odd-parity electron excited state appears as a bound state (which is hardly possible due to the small heights of these structures).

(2) An anomalous avoided crossing appears in the ground-state exciton dissociation by removal of the electron from the deeper dot (hole staying localized in the deeper dot) involving more than two energy levels. Such an effect is observed when a dark energy level with an excited hole enters the principal avoided crossings energy gap. In such a case, the hole energy levels are mixed by the electron transfer: the excited hole states acquire an admixture of the ground state of the hole and thus appear as temporarily bright levels in the avoided crossing range.

(3) A wide avoided crossing of bright and dark energy levels related to hole tunneling is observed for the field orientation opposite to the one inducing the electron interdot transfer. Contrary to the avoided crossings due to the electron tunneling, which are visible already for the ground state, the wide avoided crossing due to the hole transfer appears only for an excited state for which the hole starts to occupy both dots.

Let us comment on the potential influence of the light hole on these features. In (1), the hole remains in its lowest energy state while the electron tunnels and no influence should be expected. In (2), the mixing of the hole energy levels involves the two lowest excited hole states for which the light hole contribution should still be negligible. The contribution of the light hole, which tunnels nearly as effectively as the electron, may influence feature (3) by *enhancing* the avoided crossing.

V. CONCLUSION AND SUMMARY

We studied the electron-hole pair states in laterally coupled self-assembled quantum dots using the configuration interaction approach. Signatures of lateral coupling in the exciton spectra dependence on the external in-plane electric field were presented and compared to the vertically stacked quantum dots. The characteristic features of the spectra include formation of anomalous avoided crossing at the ground-state exciton dissociation with more than two participating energy levels, as well as additional avoided crossings of the bright energy levels corresponding to electric-field-induced resonant alignment of electron energy levels in both dots as well as to hole tunnel coupling at the hole excited energy levels.

ACKNOWLEDGMENTS

This work was supported by the EU NoE: SANDiE and the Belgian Science Policy (IAP).

[1] H. J. Krenner, M. Sabahtil, E. C. Clark, A. Kress, D. Schuh, M. Bichler, G. Absteiter, and J. J. Finley, Phys. Rev. Lett. **94**, 057402 (2005).

[2] E. A. Stinaff, M. Scheibner, A. S. Bracker, I. V. Pomonarev, V. L. Korenev, M. E. Ware, M. F. Doty, T. L. Reinecke, and D. Gammon, Science **311**, 636 (2005).

[3] A. S. Bracker, M. Scheibner, M. F. Doty, E. A. Stinaff, I. V. Pomonarev, J. C. Kim, L. J. Whitman, T. L. Reinecke, and D. Gammon, Appl. Phys. Lett. **89**, 233110 (2006).

[4] H. J. Krenner, E. C. Clark, T. Nakaoka, M. Bichler, C. Scheurer, G. Abstreiter, and J. J. Finley, Phys. Rev. Lett. **97**, 076403 (2006).

[5] W. Sheng and J.-P. Leburton, Phys. Rev. Lett. **88**, 167401 (2002).

[6] K. L. Janssens, B. Partoens, and F. M. Peeters, Phys. Rev. B **65**, 233301 (2002).

[7] B. Szafran, T. Chwiej, F. M. Peeters, S. Bednarek, J. Adamowski, and B. Partoens, Phys. Rev. B **71**, 205316 (2005).

[8] W. Chu and J. L. Zhu, Appl. Phys. Lett. **89**, 053122 (2006).

[9] M. H. Degani, G. A. Farias, and P. F. Farinas, Appl. Phys. Lett. **89**, 152109 (2006).

[10] B. Szafran, F. M. Peeters, and S. Bednarek, Phys. Rev. B **75**, 115303 (2007).

[11] M. H. Degani and M. Z. Maialle, Phys. Rev. B **75**, 115322 (2007).

[12] L. Wang, A. Rastelli, S. Kiravittaya, M. Benyoucef, and O. G. Schmidt, arXiv:cond-mat/0612701 (unpublished).
[13] M. Schmidbauer, S. Seydmohamadi, D. Grigoriev, Z. M. Wang, Yu. I. Mazur, P. Schafer, M. Hanke, R. Kohler, and G. J. Salamo, Phys. Rev. Lett. **96**, 066108 (2006).
[14] J. L. Gray, R. Hull, and J. A. Fioro, J. Appl. Phys. **100**, 084312 (2006).
[15] J. H. Lee, Zh. M. Wang, N. W. Strom, Yu. I. Mazur, and G. J. Salamo, Appl. Phys. Lett. **89**, 202101 (2006).
[16] For the $k \cdot p$, theory of multiple system of laterally and vertically coupled dots, see V. Mlinar and F. M. Peeters, J. Mater. Chem. **17**, 3687 (2007).
[17] D. Xu, N. Zhao, and J. L. Zhu, arXiv:0705.3880v1 (unpublished).
[18] We consider only the spin 1 exciton. In the following, by "bright" and "dark" we refer to the states of large and small recombination probabilities, respectively. The recombination probability is calculated as an "overlap" of the electron and hole (for the formula, see Ref. 10).
[19] The lateral coupling between the dots turns out to be much weaker than the coupling of vertically stacked dots. For our discussion, we consider only the distance between to 20 and 21 nm, i.e., for very thin interdot barrier, when the dots (of radius or side length of 20 nm) nearly merge. For larger distance, the coupling promptly vanishes.
[20] J. A. Barker and E. P. O'Reilly, Phys. Rev. B **61**, 13840 (2000).